

## CHARACTERISTICS OF THE TEMPORAL STRUCTURE OF RADIATION IN DENSE CATTERING MEDIA, II. EFFECT OF GEOMETRIC PARAMETERS OF THE EXPERIMENT AT SMALL SCATTERING ANGLES

V.V. Vergun, E.V. Genin, G.P. Kokhanenko, V.A. Krutikov, and D.S. Mezhevoi

*Institute of Atmospheric Optics,  
Siberian Branch of the Academy of Sciences of the USSR, Tomsk  
Received February 13, 1990*

*The contribution of single and multiple scattering to the spatiotemporal structure of radiation is estimated in the region of predominantly small-angle scattering (the optical thickness  $\tau = 1-20$ , zone near the axis). The broadening and exponential decay of the amplitude of the pulses as a function of the depth are investigated for different angles of observation. The effect of the angular aperture of the detector on the measurement of the width and energy of the pulse is estimated.*

In Part 1 of this work<sup>1</sup> we investigated a procedure for observing the temporal shape of pulses propagating in a scattering medium. In Part 2 we present the results of investigations of the energy attenuation and the temporal structure of the pulses. These results show that single scattering (SS) and multiple scattering (MS) of radiation are both important near the axis of the beam.

Near the axis of the beam, in a region of not too large thicknesses ( $\tau \sim 10-20$ ), the background of scattered radiation is formed predominantly by multiple scattering at small angles (the variance of the angular distribution of the photons  $\bar{\theta}^2 = \int \theta^2 J(\theta) d(\cos \theta) \ll 1$ ).

At the same time the radiation singly scattered in the volume where the beam crosses the field of view of the detector (see Fig. 1 of Ref. 1) or a straight beam that is attenuated as  $e^{-\tau}$ , if the detector is located on the axis ( $\alpha = 0^\circ$ ), makes a significant contribution to the total signal.

Comparing the experimental results<sup>1</sup> or numerical calculations with the results that are most applicable in the region of small-angle (SA) approximations,<sup>2</sup> it must be kept in mind that the small-angle approximations are constructed for the radiation brightness function (i.e., of point, monodirectional detectors), while experiments are performed with a detector with a concrete value of the area and angular aperture. The effect of the aperture (within the most widely used limits  $\omega = 0.1-1.0^\circ$ ) can significantly change the ratio of single to multiple scattering at different times and, on the whole, their contribution to the energy of the pulse.

The extinction of radiation in the straight-beam zone according to the law  $J = J \exp(-\tau)$  is observed for detectors with extremely small aperture right up to optical thicknesses  $\tau = 15-20$  (Ref. 3). For detectors with a quite wide field of view ( $\omega \sim 1^\circ$ ) multiple scattering of radiation reaching the detector must be taken into account. In the case when a covered by the objective scattering predominates and conditions

$$\bar{\theta}^2 \ll \omega^2 \ll 1 \quad (1)$$

are satisfied, the radiation scattered on any section of the path within the angles  $\theta < \omega$  is recorded by the detector. Taking this part of the radiation into account in Bouguer's law

$$\frac{dJ}{dz} = -\epsilon J + \Lambda \epsilon J \int_{\Omega} g(\theta) d\Omega, \quad (2)$$

where  $\Lambda$  is the single-scattering albedo,  $J$  is the intensity of the radiation,  $\epsilon$  is the extinction coefficient,  $g(\theta)$  is the scattering phase function, and  $z$  is the longitudinal coordinate, we obtain the exponential decay of intensity well known from the multiple-scattering approximations<sup>2</sup> for both wide and narrow beams:

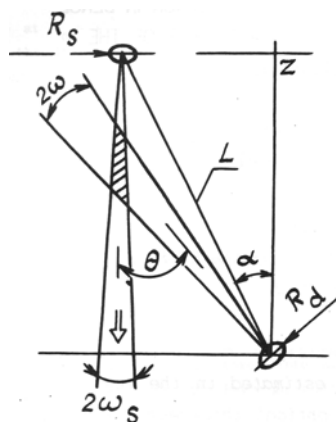


FIG. 1. Geometry of the numerical experiment.

$$J = J_0 \exp\{-\tau(1 - \Lambda\Delta)\}, \tag{3}$$

where the correction  $\Delta$  is the relative fraction of the light that is scattered in an elementary act within the field of view of the detector

$$\Delta = \int_0^{2\pi} d\varphi \int_0^\omega g(\theta) \sin\theta d\theta. \tag{4}$$

Exponential dependences of the form (3) for the intensity of light in the straight-beam zone have been observed in a number of experiments.<sup>4,5</sup>

We shall now study the case when the observations are performed off the beam axis at an angle  $\alpha \ll 1$ . Under conditions when small-angle scattering predominates (2) we can use the well-known model of the light field<sup>2</sup> that takes into account the fact that outside the straight-beam zone the energy of the multiply f-scattered radiation is determined by single scattering by a "large" angle  $\theta$  (observation angle) and by multiple scattering at small angles near the forward direction. The quasi-single-scattering approximation, which is valid for large observation angles  $\theta > \pi/2$  and appreciable absorption by the medium, is, for example, based on this model. In our case (zone near the axis of the beam,  $\alpha \ll 1$ ) singlet scattering of radiation, formed within the field of view of the objective

$$J_{ss}(\theta) \sim J_0 g(\theta) \tau \omega V / Q, \tag{5}$$

where  $V$  is the scattering volume and  $Q$  is the cross-sectional area of the beam, will appear as the source of radiation in Bouguer's law (2). This leads to a dependence of the form

$$J(\theta) \sim J_0 g(\theta) \tau \omega \exp\{-\tau(1 - \Lambda\Delta)\}, \tag{6}$$

where the correction  $\Delta$  takes into account the maximum angle of deflection of the photons striking the detector in the case of single scattering:

$$\Delta = \int_0^{2\pi} d\varphi \int_0^{\omega+\theta} g(\theta) \sin\theta d\theta. \tag{7}$$

According to the relation (6) the maximum of the signal is observed for  $\tau = 1$ .

Figure 2 (curves 1–3) shows the dependences obtained in the model experiment<sup>1</sup> for the amplitude of the signal for different polar angles  $\alpha$  in the case of observation in the direction toward the source (this corresponds to the case  $\theta = \alpha$  in Fig. 1). For the conditions of our experiment ( $\omega = 2^\circ$ , the scattering phase function is for Deirmendjian's C1 cloud) the quantity  $\Delta$  calculated using Eq. (7) is:  $\Delta = 0.4$  ( $\alpha = 0^\circ$ ),  $0.43$  ( $\alpha = 0.5^\circ$ ), and  $0.48$  ( $\alpha = 1.8^\circ$ ). The experiment shows the existence of exponential decay for  $\tau$  ranging from 2 up to 20–25, and in addition the

experimental data give a rate of decay that agrees quite well with the computed rate (the slope of the straight lines for  $\alpha = 0^\circ$  (1),  $0.5^\circ$  (2), and  $1.8^\circ$  (3) was calculated from the relation (6)).

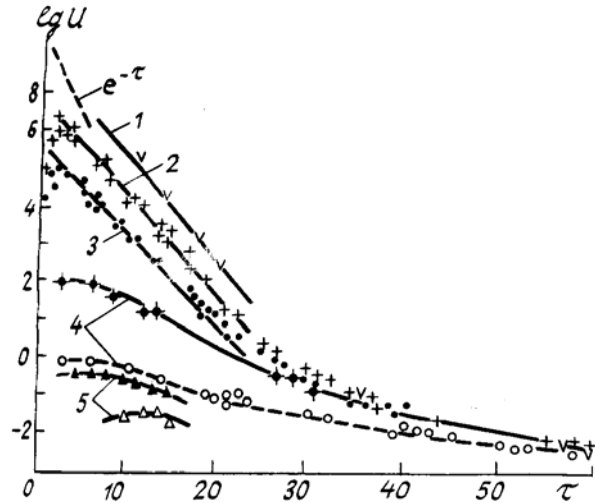


FIG. 2. The amplitude of the signals as a function of the optical thickness for different observation angles: 1)  $\alpha = 0^\circ$ , 2)  $0.5^\circ$ , 3)  $1.8^\circ$ , 4)  $\psi = 10^\circ$ , and 5)  $\psi = 65^\circ$ .

The existence of predominantly single scattering by a large angle is determined by the condition that the angular variance of multiply scattered radiation is small compared with the "large" angles  $\alpha$ ,  $\theta$ , and  $\omega$ . In the opposite case, multiple scattering by large angles starts to make a significant contribution, and the expression (6) is no longer valid. When the geometry of the experiment is constant this limits the region of exponential decay on the side of large  $\tau$ . Characteristically, for the depolarized component, formed by multiple scattering by large angles, the region of exponential decay is not observed. This region also vanishes when the detector is removed from the meridional plane. Figure 2 shows the dependence of the amplitudes of the signal for the azimuth  $\psi = 10^\circ$  (curves 4) and  $\psi = 65^\circ$  (curves 5) for the angle  $\alpha = 1.8^\circ$ . The depolarized component is indicated by a dashed line, and for  $\tau > 15$  the data for  $\psi = 0^\circ$  coincide with the data for  $\psi = 10^\circ$ .

The increase in the effective multiplicity of scattering by large angles is manifested in the fact that the maximum is displaced toward large values of  $\tau$  (thus, for  $\psi = 65^\circ$  it is observed at  $\tau = 5$  for  $J_{||}$  and  $\tau = 12$  for  $J_{\perp}$ ) and there is no zone of exponential decay.

The temporal structure of the radiation in the region of optical thicknesses of interest to us also depends on the angular characteristics of the experiment. Figure 3 shows the results of measurements of the pulse width for different observation angles  $\psi$ . The data obtained by processing the signals by the method of regularization are plotted with a margin of  $\pm 1$  ns, corresponding to the accuracy of the method for

the observed noise level. For the other data the well-known property of convolution was employed: the variance of the recorded pulse  $\overline{\Delta t_{rec}^2}$  is equal to the sum of the variances of the starting pulse and the ITF. The fact that the application of an analogous expression to the usually determined parameter — the width of ITF at half amplitude

$$\Delta t^2 = \Delta t_{rec}^2 - \Delta t_0^2$$

is justified only for large values of  $\tau$ , where the pulse shape is quite stable but leads to a significant (by 2 to 3 ns) overestimation of the width of the ITF for  $\tau = 10-20$ , must be taken into account.

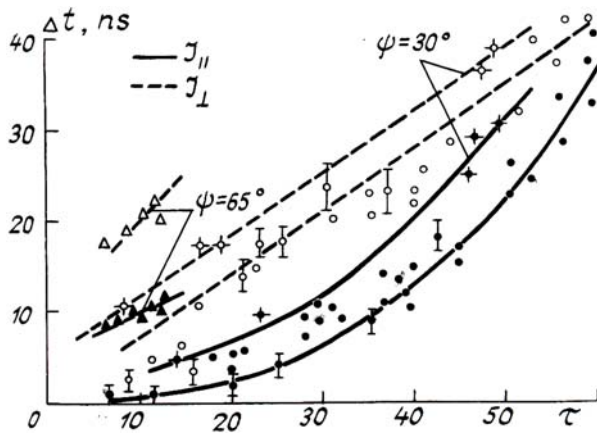


FIG. 3. The pulse width versus the optical thickness of the layer.

The dependence of the width of the scattered pulse on the observation angle  $\psi$  can be clearly traced (right up to  $\tau = 50$ ), and it is obvious that the character of the dependence  $\Delta t(\tau)$  for the polarized component of the pulse is different from that of the cross-polarized component.

The limited resolution time of the model experiment leads to large errors in the determination of the form of the ITF of the medium for the total signal ( $J_{||}$ ) for  $\tau < 20$ . This could be why the difference in the shape of the pulse for observations in the direction toward the source ( $\psi = 0$ ) at different distances from the axis ( $\alpha = 0-2^\circ$ ), which could exist in the region of small-angle scattering ( $\tau < 20$ ), was not observed. In studying the temporal structure of the signal it is especially important to study the contribution of single and multiple scattering of radiation, since the parameters of the experiment affect them differently. The temporal structure of multiple scattering of radiation depends on both the angular parameters of detection and the optical thickness of the medium. The duration of the singly scattered signal is determined solely by the geometric parameters and for small  $\theta$  and  $\omega$  it can be estimated as (see Fig. 1)

$$\Delta t \approx \frac{1}{2} \frac{Z}{c} \alpha \omega. \tag{8}$$

Based on the above-noted restrictions on the experiment, we performed numerical calculations by the Monte Carlo method. The numerical experiment was performed in the geometry shown in Fig. 1 for the case when the detector is oriented in the direction toward the source ( $\theta = \alpha$ ), the path length  $Z = 6000$  m, and the scattering layer uniformly fills the space  $0-Z$ . The model of a C1 cloud for  $\lambda = 0.45 \mu\text{m}$  was employed.

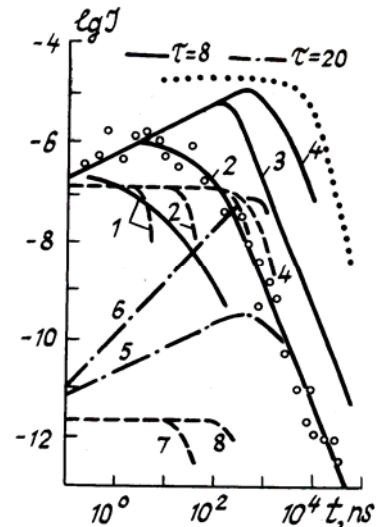


FIG. 4. The form of the pulses for different angular apertures of the detector for the angle  $\alpha = 10^\circ$ : 1)  $\omega = 0.1^\circ$ , 2, 5)  $\omega = 1^\circ$ , 3, 6)  $\omega = 10^\circ$ , and 4)  $\omega = 80^\circ$ . The dashed lines are for single scattering.

Figure 4 shows the computational results for the signal intensity for optical thickness  $\tau = 8$  and detectors with different angle of the field of view with the slope angle  $\alpha = 10^\circ$  with respect to the axis. The dashed curves correspond to single scattering and the solid curves correspond to multiple scattering. Initially the signal formed by photons with a small angular spectrum is identical for all detectors and close to the intensity of the singly scattered radiation. At long times the angular dispersion of the scattered photons increases, and as a result for detectors with a large viewing angle the intensity of the maximum increases and the maximum is delayed in time. The intensity of the singly scattered radiation remains the same, but the duration of this radiation and therefore the energy increase according to the relation (8) as the field of view increases. If for  $\omega = 0.1^\circ$  (curve 1) the intensity of the multiply scattered radiation at the maximum is equal to the intensity of the singly scattered radiation and exceeds it only on the trailing edge of the pulse, then for large angles of the field of

view the energy of the pulse is determined entirely by multiple scattering, which at the maximum is an order of magnitude higher than the single scattering for  $\omega = 1^\circ$  (2). In addition, in the entire range of angular apertures of the detector the time of arrival of the maximum of the multiply scattered radiation does not exceed the width of the single scattered pulse, which is determined in accordance with the relation (8) and does not depend on  $x$ ; this in turn indicates that the conditions for small-angle scattering (1) are satisfied.

For comparison Fig. 4 shows (dots) the asymptotic time dependence (the amplitude is plotted in arbitrary units).<sup>5</sup> The duration of the multiply scattered radiation will exceed the singly scattered radiation when the conditions (1) are not satisfied, i.e., when the effective multiplicity of the scattering at "large" angles, comparable to  $a$  and  $u$ , increases. If the geometry of the experiment does not change, this will occur as the optical thickness  $\tau$  increases.

The calculation of the pulse shape for  $\tau = 20$  for two angles of the field of view  $\omega$  is also presented in Fig. 4 by the dot-dashed curves. The broadening of the pulse compared with the singly scattered pulse is especially large for  $\omega = 1^\circ$  (curve 5), and in this case the maximum of the signal is shifted relative to the singly scattered radiation by an order of magnitude. For  $\omega = 10^\circ$  (6) the maximum of the signal also crossed the boundary of the width of the singly scattered signal. The temporal characteristics of signals for different  $u$  (curves 5 and 6) in the region of the maximum are practically identical; this indicates that the angular width of the beam of multiply scattered radiation reaches a definite value when  $\bar{\theta}^2 > \omega^2$ .

However a similar situation can also occur with much smaller optical thicknesses in the case of very small  $\alpha$  and  $\omega$ .

Figure 5 shows the form of the pulses for  $\tau = 3.9$  and  $\alpha = 0.1^\circ$  for angles of field of view ranging from  $\omega = 0.001^\circ$  (curve 1) to  $\omega = 1^\circ$  (curve 4). The amplitude of the multiply scattered radiation is proportional to  $\omega^2$  (indicating that the multiply scattered radiation is isotropic within a range of  $1^\circ$ ) and the width of the multiply scattered pulse also does not change. At  $\omega = 1^\circ$  the multiply scattered radiation contributes 87% of the total energy of the signal. In this situation the approximate solutions, describing well the multiply scattered radiation, will describe quite correctly the shape of the total signal. However already for  $\omega = 0.01^\circ$  the width of the multiply scattered pulse is an order of magnitude larger than the width of the singly scattered pulse, and the contribution of the multiply scattered radiation to the energy drops to 10%. The total signal will be determined predominantly by the singly scattered radiation. Thus reducing the angular aperture of the detector in this region of geometric parameters no longer improves the agreement between the experiment and the small-angle approximations.

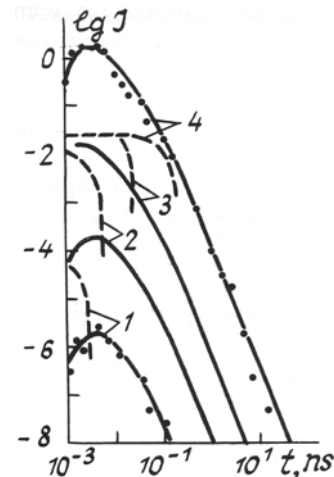


FIG. 5. The shape of the pulses for different angular apertures of the detector for  $\alpha = 0.1^\circ$ : 1)  $\omega = 0.001^\circ$ , 2)  $\omega = 0.01^\circ$ , 3)  $\omega = 0.1^\circ$  and 4)  $\omega = 1^\circ$ .

The results presented in this paper show the quite complicated spatiotemporal structure of the scattered background in the region of the transitional optical thicknesses  $1 < \tau < 20$ . The mutual contribution of the singly and multiply scattered radiation depends significantly on the geometric parameters of the detector. In the limiting cases with  $\bar{\theta}^2 \ll \omega^2$ , the width of the signal is determined by single scattering (even for  $\tau \approx 10$ ), while for  $\bar{\theta}^2 \gg \omega^2$  the width does not depend on  $\omega$  and the pulse energy  $\sim \omega^2$ . For most approximate solutions of the radiation transfer equation, which do not take these factors into account, the additional limits of applicability of the solutions and an appropriate procedure for comparing the numerical results with experiment must be determined.

## REFERENCES

1. V.V. Vergun, E.V. Genin, G.P. Kokhanenko, V.A. Krutikov, and D.S. Mezhevoi, *Atm. Opt.* **3**, No. 7, 691 (1990).
2. E.P. Zege, A.P. Ivanov, and I.L. Katsev, *Image Transfer in a Scattering Medium* [in Russian] (Nauka i Tekhnika, Minsk, 1986).
3. V.E. Zuev and M.V. Kabanov, *Transfer of Optii Signals in the Earth's Atmosphere (Under Noisy Conditions)* (Sov. Radio, Moscow, 1977).
4. V.E. Zuev, M.V. Kabanov, and B.A. Savel'ev, *Dokl. Akad. Nauk SSSR* **175**, No. 2, 327 (1967).
5. Yu.A. Gol'din, V.V. Bacherikov, et al. *Hydrophysical and Optical Investigations in Indian Ocean* (Nauka, Moscow, 1975).
6. V.V. Ivanov and S.D. Gutshabash, *Izv. Akad. Nauk SSSR, Ser. FAO* **10**, No. 8, 851 (1974).